Sparsity Signal Detection for Indoor GSSK-VLC System

Ting Zuo, Fasong Wang, Jiankang Zhang, *Senior Member, IEEE*

Abstract—In this paper, the signal detection problem in indoor visible light communication (VLC) system aided by generalized space shift keying (GSSK) is modeled as a sparse signal reconstruction problem, which has lower computational complexity by exploiting the sparse reconstruction algorithms in compressed sensing (CS). In order to satisfy the measurement matrix property to perform sparse signal reconstruction, a preprocessing approach of measurement matrix is proposed based on singular value decomposition (SVD), which theoretically guarantees the feasibility of utilizing CS based sparse signal detection method in indoor GSSK-VLC system. Then, by adopting classical orthogonal matching pursuit (OMP) algorithm and compressed sampling matching pursuit (CoSaMP) algorithm, the GSSK signals are efficiently detected in the considered indoor GSSK-VLC system. Furthermore, a more efficient detection algorithm combined with OMP and maximum likelihood (ML) is also presented especially for SSK scenario. Finally, the effectiveness of the proposed sparsity aided detection algorithms in indoor GSSK-VLC system are verified by computer simulations. The results show that the proposed algorithms can achieve better bit error rate (BER) and lower computation complexity than ML based detection method. Specifically, a signal-to-noise ratio (SNR) gain as high as 12 dB is observed in the SSK scenario and about 5 dB in case of a GSSK scenario upon employing our proposed detection methods.

Index Terms—Visible light communication (VLC), generalized space shift keying (GSSK), compressed sensing (CS), maximum likelihood (ML), signal detection.

I. Introduction

AS a promising new communication technology in wireless communication system, visible light communication (VLC) has many unique advantages compared with traditional radio frequency (RF) communication, such as rich spectrum resources, good confidentiality, no license requirements, anti-electromagnetic interference, etc. [1], [2]. The research on VLC has aroused strong interest of researchers in various fields from both academia and industry. The combination of VLC and multiple-input multiple-output (MIMO) technology can significantly improve the transmission rate and performance of the communication system [3]. Based on these advantages, MIMO transmission in indoor VLC has been widely studied in recent years.

T. Zuo and F. Wang are with the School of Information Engineering, Zhengzhou University, Zhengzhou, 450001, Henan, China. (E-mails: 15978370982@163.com, iefswang@zzu.edu.cn)

J. Zhang is with the Department of Computing and Informatics, Bournemouth University, Bournemouth BH12 5BB, U.K. (e-mail: jzhang3@bournemouth.ac.uk)

Spatial modulation (SM), as a simple and efficient MIMO scheme, has been widely studied in the last decade. It utilizes the active antenna index to convey additional information and achieves effective improvement of spectral efficiency (SE) [4]. The latest and detailed research results of SM technology in recent years was described in [5]. Furthermore, some extended schemes based on SM have been proposed to improve the performance of the application systems in [6]–[13]. Specifically, space shift keying (SSK) is one of the SM technologies with the lowest device complexity and the easiest implementation [6], which employs only spatial symbols to convey information. Then, to improve the SE of systems, the generalized SSK (GSSK) [7] and generalized SM (GSM) [8] schemes were proposed by activating multiple transmitting antennas simultaneously. Different from traditional SM that employs the index of transmitting antenna to transmit information, by exploiting the index of receiving antenna to convey spatial information, a pre-coding SM scheme was proposed in [9], [10]. Then, by extending the spatial symbols to in-phase components and orthogonal components, the spatial SE of quadrature SM (QSM) technology is doubled compared with traditional SM, and the bit error rate (BER) of the system can also be improved [11]–[13]. Furthermore, based on these advantages of QSM technology, a generalized pre-coding QSM (GPQSM) scheme was proposed in [12], the authors also proved that GPQSM scheme was superior to traditional GPSM scheme at the same SE. Additionally, practical application of GQSM combined with NOMA technology was designed in vehicle collaborative networks [13]. Actually, as one of the successful multiple antenna technologies in RF based wireless communication systems, GSSK has been extensively studied due to its less cost, fewer RF links and lower complexity [14]. SSK is one of the GSSK technologies with the lowest device complexity and the easiest implementation. In practice, for the limited luminous flux of an individual light-emitting diodes (LED) and the size of a typical room, multiple LEDs are usually utilized for obtaining adequate illumination. When multiple LEDs are activated to transmit information, these spatially distributed LEDs can be exploited for implicitly conveying information. Therefore, the GSSK scheme is also suitable for VLC systems [15], [16]. Furthermore, the advantages and disadvantages of GSSK technology in indoor VLC system have been thoroughly analyzed, the authors of [16] pointed out that GSSK is suitable for the situation where the receiver position is fixed, because the mobility of the receiver greatly affects its performance. In order to enhance the error performance of the traditional GSSK-VLC system, a low-complexity power allocation scheme was proposed in the direct-coded GSSK system, which improved the symbol error rate while increasing the transmission rate [17]. For the indoor VLC system based on GSSK, the physical layer

security problem was considered in [18], [19], the security performance of the system was analyzed, and the methods of security improvement based on LEDs selection and artificial noise injecting were also proposed.

The detection methods in the above-mentioned indoor GSSK-VLC system are mainly based on the maximum likelihood (ML) method. Although the detection performance is optimal, the computational complexity brought by exhaustive search will increase dramatically when the number of LEDs at the transmitter is large. Therefore, it is very important to find a detection scheme with low complexity and a lower BER at the receiver. Linear detection algorithms, such as zero forcing (ZF) and minimum mean error (MMSE), have a significant complexity reduction compared with ML, but at the expense of error increasing. Furthermore, these two approaches are only applicable to the over-determined systems [20]. Recently, a low complexity logarithmic likelihood ratio (LLR) detection algorithm is employed in the joint mapping non-orthogonal frequency division multiplexing with subcarrier number modulation (JM-OFDM-SNM) scheme in [21]. Compared with ML, the LLR detector scheme has no obvious attenuation in performance, while the detection complexity is significantly reduced. Inspired by this, the LLR detector may be applicable to our considered GSSK-VLC system, but it needs further investigation to integrate them.

Practically, multiple LEDs are utilized for satisfying adequate illumination, and by GSSK modulation, only several LEDs are activated to transmit information. Therefore, the transmitted information signals have inherent sparsity. Consequently, by considering the sparse characteristics of GSSK signals in GSSK-VLC system, the sparse signal reconstruction method in compressed sensing (CS) theory can provide ideal balance between the computational complexity and the system error performance. As an innovative theory of signal acquisition, encoding and decoding, CS was proposed by Donoho *et al.* [22], among which greedy algorithm is one of the main algorithms involved in sparse signal reconstruction. The greedy algorithm includes orthogonal matching pursuit (OMP) and a series of improved algorithms of OMP [23], [24].

The application of CS theory in GSSK aided RF communication system has been extensively studied [25]–[29]. Specifically, a normalized CS algorithm was applied to demodulate GSSK signals in RF communication system by utilizing the OMP algorithm in [25]. Then, in order to improve the system performance, an equalizer based on OMP algorithm was applied to the receiver to make the equivalent channel matrix orthogonal [26]. Following this, by increasing the iteration number, a modified OMP algorithm in GSSK system was proposed to improve system performance, however in high signal-to-noise ratio (SNR) condition, flooring effect will appear [27]. Then, a new sparse reconstruction algorithm for detecting GSSK signals was proposed to enhance system performance compared with existing CS based detection algorithms in [28]. Different from the traditional CS algorithm, which uses inner product operation to find matching atoms, a new atomic matching criterion based on Euclidean distance was proposed in [29], which improves both the performance and complexity of the algorithm. With respect to the applications of CS

technology in VLC system, indoor positioning was considered in [30], [31], while the experimental demonstration of CS based channel estimation for MIMO-OFDM VLC was given in [32].

To the best of our knowledge, there are no research results in the open literature on the comprehensive usage of GSSK-VLC system relying on CS based sparse signal reconstruction algorithm for signal detection, which inspired this treatise.

Motivated by the aforementioned issues, in this paper, we propose and study the signal detection problem in indoor GSSK-VLC system. In particular, we analyze the channel characteristics of indoor GSSK-VLC system, by utilizing a preprocessing approach to the measurement matrix of the CS aided system model, a series efficient sparse reconstruction algorithms are proposed to achieve signal detection. The contributions of this paper can be summarized as follows:

- Unlike the channel matrix in traditional RF communication, which approximately meets the restricted isometric property (RIP) in CS theory, *the elements of channel matrix of indoor VLC system are almost fixed value determined by the locations of receiver and transmitter, and other system parameters. And consequently, it makes the measurement matrix always not meet the RIP characteristics*, which is the prerequisite for the effective use of CS algorithm. Therefore, aided by this conclusion, *a preprocessing approach on the channel matrix is proposed based on singular value decomposition (SVD), which theoretically guarantees the feasibility of utilizing CS based sparse signal reconstruction method in indoor GSSK-VLC system.*

- In order to enhance the detection efficiency of ML method, by adopting classical OMP method and compressed sampling matching pursuit (CoSaMP) method, *an efficient GSSK signal detection algorithm framework is proposed* in the considered indoor GSSK-VLC system. Additionally, *a more efficient detection algorithm combined with OMP and ML is also presented especially for SSK scenario. Compared with ML, these detection algorithms reduce the computational complexity dramatically and improve the BER performance obviously*. Specifically, a SNR gain as high as 12 dB is observed in the SSK scenario and about 5 dB in case of a GSSK scenario upon employing our proposed detection methods.

The rest of this paper is arranged as follows: in section II, the model of indoor GSSK-VLC system is described in detail. In Section III, the CS aided detection algorithms are proposed for the considered indoor GSSK-VLC system. The parameter setting and detailed simulation experiments are provided in section IV. Finally, we conclude the whole paper in section V.

II. SYSTEM MODEL

A. Channel Model of Indoor VLC

In the indoor VLC system, the LEDs serve as the transmitter to provide lighting and conduct high-speed short-range communication simultaneously [33], and the receiver receives signals with photo-detectors (PDs). The transmitter of indoor VLC system is equipped with N_t LEDs and the number of PDs

at the receiver is N_r. In this paper, intensive modulation/direct detection (IM/DD) is considered. In the system considered, it is further assumed that all LEDs are used to perform illumination and the lighting power is I. The activated LEDs implement IM to transmit information to accomplish communication, and the emitted symbol with an intensity of $I_m \in \mathbb{M}$, where $\mathbb{M}$ is the set of all possible emission signal intensity levels. I_m can be expressed as: $I_m = \frac{2I_p m}{M+1}, m = 1, 2, \ldots, M$, where M represents the order of intensity modulation, I_p represents the average optical power of the transmitted signal, and non-activated LEDs are only utilized for illumination.

Fig. 1 depicts a typical indoor VLC model with a room size of 5 m $\times$5 m $\times$3 m. The LEDs are 0.5 m away from the ceiling and the PDs are placed on a plane 0.8 m away from the ground. Due to the light propagation characteristics, the signals received by the receiver of indoor VLC system include line of sight (LOS) component and non-LOS (NLOS) components [19]. LOS means that the signal sent by LEDs is directly received by PD, while NLOS denotes the optical signal sent by LEDs reaches the receiver after refraction or reflection by the object. Because NLOS contains very little optical power, only LOS transmission channel is considered in this paper [34]. Assuming further that the LED has a generalized Lambert emission mode, Fig. 2 shows the geometric model of LOS transmission, where ϕ and θ are the angle of emergence and incidence at the PD, respectively. Furthermore, FOV is the field-of-view (FoV) semi-angle of the detector, and $\Phi_{1/2}$ is the half power semi-angle of LED, d is the distance between transmitter and receiver.

Fig. 2. Geometric model of LOS path in indoor VLC system

$\mathbf{H}$ with dimensional $N_r \times N_t$ can be expressed as

$$\mathbf{H} = \begin{bmatrix} h_{11} & h_{12} & \ldots & h_{1N_t} \\ h_{21} & h_{22} & \ldots & h_{2N_t} \\ \vdots & \vdots & h_{ij} & \vdots \\ h_{N_r 1} & h_{N_r 2} & \ldots & h_{N_r N_t} \end{bmatrix} \quad (2)$$

where h_{ij} represents the channel gain between the jth LED and the ith PD. In summary, the input-output relationship of the indoor VLC channel between the N_t LEDs and the N_r PDs can be modelled as

$$\mathbf{y} = \mathbf{H}\mathbf{x} + \mathbf{n} \quad (3)$$

where $\mathbf{x} = [x_1, x_2, \cdots, x_{N_t}]^{\mathrm{T}} \in \mathcal{R}^{N_t}$ is an information-bearing signal vector sent by LEDs, and $\mathbf{y} = [y_1, y_2, \cdots, y_{N_r}]^{\mathrm{T}} \in \mathcal{R}^{N_r}$ is the received signal vector by PDs. Finally, $\mathbf{n} \sim \mathcal{N}(0, \sigma^2)$ is zero-mean additive white Gaussian noise (AWGN) processes vector received by PDs.

B. GSSK Modulation in Indoor VLC System

Assuming that there are N_t LEDs in the considered service area. For the proposed GSSK-VLC system, only N_a ($1 \leq N_a \leq N_t$) out of the N_t LEDs are activated to simultaneously transmit their information by exploiting GSSK modulation, while the remaining $(N_t - N_a)$ LEDs are only employed for illumination. Hence, there are totally $M = \binom{N_t}{N_a}$ possible combinations, among which $2^{\eta_{\mathrm{GSSK}}}$ with $\eta_{\mathrm{GSSK}} = \lfloor \log_2 M \rfloor$ are used transmitting η_{GSSK} bits per symbol, $\lfloor \cdot \rfloor$ denotes floor operation. In our following discussions, we explicitly select the first $2^{\eta_{\mathrm{GSSK}}}$ combinations for conveying information. As a special GSSK modulation, SSK is the simplest case of GSSK, where only one LED is activated in each time slot, and information is transmitted only depending on the index of the single activated LED. Therefore, the number of bits of information transmitted by SSK in each time slot is $\eta_{\mathrm{SSK}} = \lfloor \log_2(N_t) \rfloor$. Hence, all the following results can be straightforwardly applied to indoor SSK-VLC system by letting $N_a = 1$.

In summary, the system model of the GSSK scheme is illustrated in Fig. 3 with configuration $N_t = 4, N_a = 2$, thus a GSSK symbol carries $\eta_{\mathrm{GSSK}} = 2$ bits of information. As an demonstration, the mapping criterion between activated
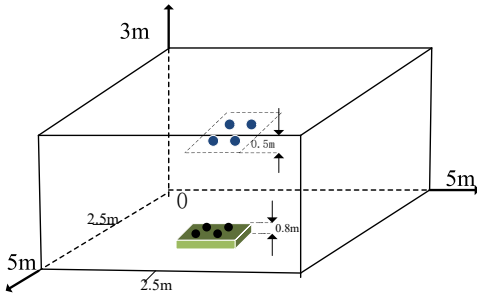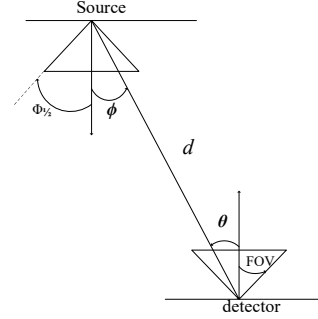

Fig. 1. Indoor VLC system model with $N_t = 4, N_r = 4$

Then the channel gain between LED and PD can be expressed as [35]

$$h = \frac{A(k+1)}{2\pi d_{ij}^2} (\cos \phi)^k \cos \theta \, \mathrm{rect}\left(\frac{\theta}{\mathrm{FOV}}\right) \quad (1)$$

where A is the area of PD, and k is the mode number of the radiation lobe, which can be expressed as $k = -\ln(2)/\ln\left(\cos(\Phi_{1/2})\right)$, $\mathrm{rect}(\cdot)$ function indicates that PD cannot receive optical signal when the incident angle of PD is greater than FOV, and the channel gain h between LED and PD is 0 in this case. Then the optical MIMO channel matrix

LEDs combination and transmission information bits can be defined as follows: $(1,2) \rightarrow [0,0], (1,3) \rightarrow [0,1], (1,4) \rightarrow [1,0], (2,3) \rightarrow [1,1]$, where the symbol (n_i, n_j) represents the index of activated LEDs, where $n_i \neq n_j$ and $n_i, n_j = 1, 2, \cdots, N_t$, and the symbol $[m_i, m_j]$ represents the information bits with elements $m_i, m_j = 0$ or 1. Since GSSK only uses the combination of activated antennas to send information, it may as well assume that the symbol intensity of all transmitted is identical and equals to 1. Hence, all possible transmitted signal vectors can be expressed in the following matrix with each column a possible information conveying signal vector as

$$\mathbb{X} = [\mathbf{x}_1, \mathbf{x}_2, \mathbf{x}_3, \mathbf{x}_4] = \begin{bmatrix} 1 & 1 & 1 & 0 \\ 1 & 0 & 0 & 1 \\ 0 & 1 & 0 & 1 \\ 0 & 0 & 1 & 0 \end{bmatrix} \quad (4)$$
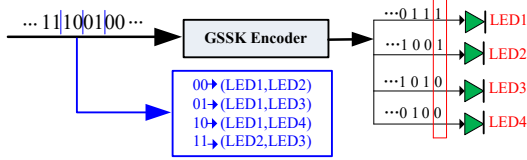

Fig. 3. Demonstration of the considered GSSK-VLC system with configuration $\eta_{\text{GSSK}} = 2, N_t = 4, N_a = 2$

III. PROPOSED PREPROCESSING AND DETECTION ALGORITHMS IN GSSK-VLC SYSTEM

CS theory shows that when the signal is sparse in a certain transformation domain, it can be compressed by a reasonably designed measurement matrix, and then the original high-dimensional signal can be recovered by sparse reconstruction algorithm [22]. This idea has been widely exploited in the field of signal processing [22]–[24]. The most significant aspect of CS theory is it can compress the signal simultaneously in the process of sampling, and is not limited by the Nyquist sampling theorem, which greatly reduces the cost of data storage and transmission [22]. In this paper, a class of signal detection approaches of the considered GSSK-VLC system are designed by employing sparse reconstruction algorithm based on CS theory. In our considered MIMO GSSK-VLC system, the proposed detection algorithm can achieve better BER performance and lower computation complexity than ML based detector.

However, CS aided sparse reconstruction algorithm has some limitations when applied to reconstruct the original signals accurately in applications. On the one hand, the original signals should be sparse or can be made sparse by proper transformations; On the other hand, the measurement matrix of the system should meet the RIP property, which is the premise of the utilization of CS based sparse reconstruction algorithm. Thus, the design of the measurement matrix

affects directly the quality of the reconstructed signal, and so the detection accuracy. In our considered GSSK-VLC system, the original signals have inherent sparsity property, hence, how to design the desired measurement matrix with RIP property is a major challenge.

According to CS theory, in order to accurately recover the original transmitted signal $\mathbf{x}$, the measurement matrix $\mathbf{H}$ needs to meet the RIP property. In RF communication, the elements in channel matrices are usually Gaussian random variables, and it has been shown that such matrices can satisfy the RIP property with a high probability [36]. In our considered GSSK-VLC system, whether the elements of measurement obey the Gaussian random distribution cannot be determined directly [37]. In order to investigate the RIP property of measurement matrix in the considered system, a hypothesis test approach, termed as the Jarque-Bera test [38], is executed to test the hypothesis that the distribution of the channel gain random variables is a Gaussian distribution at the 5% significance level. Based on the channel matrix model in section II and simulation parameter settings in Section IV, the test always returns a value of 1, which means that the elements of the measurement matrix do not obey the Gaussian distribution. Additionally, the simulation results depicted in Fig. 4 also confirmed that the CS aided sparse signal reconstruction algorithms could not be utilized directly. To resolve this issue, a preprocessing method of measurement matrix is proposed in this paper. By exploiting this preprocessing operation, a series signal detection algorithms based on sparsity are further proposed.

A. SVD Aided Preprocessing of Measurement Matrix

In this subsection, the measurement signal model (3) is considered. In order to facilitate the analysis, the influence of noise is not considered in the analysis process [22], [36].

Theorem 1: Suppose $\tilde{\mathbf{H}}$ is obtained by selecting N_r rows uniformly at random from $N_t \times N_t$ orthonormal matrix and the columns of $\tilde{\mathbf{H}}$ are renormalized so that they are unit-normed. Then $\tilde{\mathbf{H}}$ presents an incoherent measurement and the RIP of measurement $\tilde{\mathbf{H}}$ holds with overwhelming probability [37].

Proof: The detailed proof can be found in Section 3.4 in [37]. ∎

Theorem 2: For the channel matrix of the considered indoor GSSK-VLC system model, an SVD aided preprocessing makes the measurement matrix (channel matrix) satisfy RIP property in CS.

Proof: For the characteristics of the considered indoor GSSK-VLC system, without loss of generality, we assume that the measurement matrix $\mathbf{H} \in \mathbb{R}^{N_r \times N_t}$ satisfies full row rank, then it can be decomposed as

$$\mathbf{H} = \mathbf{U}[\boldsymbol{\Delta}, \mathbf{O}]\mathbf{V}^T \quad (5)$$

where $\mathbf{U} \in \mathbb{R}^{N_r \times N_r}, \mathbf{V} \in \mathbb{R}^{N_t \times N_t}$ are orthogonal matrices, $\boldsymbol{\Delta} = \text{diag}[\delta_1, \delta_2, \cdots, \delta_{N_r}]$, and $\delta_1 \geq \delta_2 \geq \cdots \geq \delta_{N_r} \geq 0$ are the singular values of $\mathbf{H}$, $\mathbf{O} \in \mathbb{R}^{N_r \times (N_t - N_r)}$ is a zero matrix.

Next, let $\boldsymbol{\Delta}^* = \text{diag}[\frac{1}{\delta_1}, \frac{1}{\delta_2}, \cdots, \frac{1}{\delta_{N_r}}]$, then we define the vector $\mathbf{y}_{\text{SVD}}$ as

$$\mathbf{y}_{\text{SVD}} = \boldsymbol{\Delta}^* \mathbf{U}^T \mathbf{y} = \boldsymbol{\Delta}^* \mathbf{U}^T \mathbf{H} \mathbf{x} \quad (6)$$

Let $\mathbf{Z} = \boldsymbol{\Delta}^*\mathbf{U}^T\mathbf{H}$, which is a partial orthogonal matrix and we get

$$\mathbf{y}_{\text{SVD}} = \mathbf{Zx} \qquad (7)$$

Furthermore, by utilizing (5), $\mathbf{Z}$ can be simplified as

$$\mathbf{Z} = \boldsymbol{\Delta}^*\mathbf{U}^T\mathbf{H} = \boldsymbol{\Delta}^*\mathbf{U}^T\mathbf{U}[\boldsymbol{\Delta}, \mathbf{O}]\mathbf{V}^T = [\mathbf{I}^{N_r \times N_r}, \mathbf{O}]\mathbf{V}^T \qquad (8)$$

Additionally, the preprocessed measurement matrix $\mathbf{H}_{\text{SVD}}$ is defined by $\mathbf{Z}$ as

$$\mathbf{H}_{\text{SVD}} = \mathbf{Z}\begin{bmatrix} \frac{1}{\|\mathbf{z}_1\|} & 0 & \cdots & 0 \\ 0 & \frac{1}{\|\mathbf{z}_2\|} & \cdots & 0 \\ \vdots & \vdots & \ddots & \vdots \\ 0 & 0 & \cdots & \frac{1}{\|\mathbf{z}_{N_t}\|} \end{bmatrix} = \mathbf{Z}\boldsymbol{\Upsilon} \qquad (9)$$

where $\mathbf{z}_1, \mathbf{z}_2, \cdots, \mathbf{z}_{N_t}$ is the column vector of the matrix $\mathbf{Z}$, $\|\cdot\|$ is the Euclidean norm of the vector. Follwing this, we can obtain

$$\mathbf{Z} = \mathbf{H}_{\text{SVD}}\begin{bmatrix} \|\mathbf{z}_1\| & 0 & \cdots & 0 \\ 0 & \|\mathbf{z}_2\| & \cdots & 0 \\ \vdots & \vdots & \ddots & \vdots \\ 0 & 0 & \cdots & \|\mathbf{z}_{N_t}\| \end{bmatrix} = \mathbf{H}_{\text{SVD}}\boldsymbol{\Xi} \qquad (10)$$

Finally, we can arrive at the transformed representation of the preprocessed signal as

$$\mathbf{y}_{\text{SVD}} = \mathbf{Zx} = \mathbf{H}_{\text{SVD}}\boldsymbol{\Xi}\mathbf{x} = \mathbf{H}_{\text{SVD}}\mathbf{x}_{\text{SVD}} \qquad (11)$$

where

$$\mathbf{x}_{\text{SVD}} = \boldsymbol{\Xi}\mathbf{x} \qquad (12)$$

It can be seen that (12) has two advantages: On the one hand, as a scaled version of $\mathbf{x}$, $\mathbf{x}_{\text{SVD}}$ maintains the same sparsity as $\mathbf{x}$; On the other hand, $\mathbf{H}_{\text{SVD}}$ is a partial orthogonal matrix, from Theorem 1, it satisfies the RIP property. ∎

Hence, once solving the sparse optimization problem and correctly reconstructing $\mathbf{x}_{\text{SVD}}$, the original information signal can be obtained as

$$\hat{\mathbf{x}} = \boldsymbol{\Upsilon}\mathbf{x}_{\text{SVD}} \qquad (13)$$

B. Signal Detection Algorithms Aided by Sparsity

CS reconstruction algorithms are commonly divided into two categories: convex optimization algorithm and greedy algorithm. The reconstruction performance of convex optimization algorithm is always good; however, its computation complexity is high, which restricts its applications in some special cases. As a suboptimal sparse signal reconstruction approach, the greedy algorithm selects the most matching atom and iterates until it is close to the original sparse signal, among them OMP algorithm [23] and CoSaMP algorithm [24] are two most popular and efficient greedy algorithms. For the signal detection issue in the considered indoor GSSK-VLC system, by utilizing the proposed SVD aided preprocessing method, the classical OMP and CoSaMP algorithms will be firstly adopted to reconstruct the original sparse signal. For

TABLE I
OMP ALGORITHM IN GSSK-VLC

Input:	$\mathbf{H}, \mathbf{y}, N_a$
Output:	Λ
1.	$\mathbf{r}_0 \leftarrow \mathbf{y}, t \leftarrow 0, \Lambda_0 \leftarrow \varnothing, \mathbf{A}_0 \leftarrow \varnothing$
2.	while $t \leq N_a$ do
3.	$\mathbf{p} \leftarrow \mathbf{H}^T\mathbf{r}^{(t-1)}, \mathbb{S}_t \leftarrow \arg\max(\mathbf{p})$
4.	$\Lambda_t = \mathbb{S}_t \cup \Lambda_{t-1}, \mathbf{A}_t = \mathbf{H}_{\Lambda_t} \cup \mathbf{A}_{t-1}$
5.	$\hat{\mathbf{x}}_t = \arg\min \| \mathbf{y} - \mathbf{A}_t\mathbf{x} \|_2^2 = (\mathbf{A}_t^T\mathbf{A}_t)^{-1}\mathbf{A}_t^T\mathbf{y}$
6.	$\mathbf{r}_t = \mathbf{y} - \mathbf{A}_t\hat{\mathbf{x}}_t$
7.	end while

TABLE II
COSAMP ALGORITHM IN GSSK-VLC

Input:	$\mathbf{H}, \mathbf{y}, N_a$
Output:	Λ
1.	$\mathbf{r}_0 \leftarrow \mathbf{y}, t \leftarrow 0, \Lambda_0 \leftarrow \varnothing, \mathbf{A}_0 \leftarrow \varnothing$
2.	while $t \leq N_a$ or $\| \mathbf{r} \|_2 \leq \zeta$ do
3.	$t \leftarrow t + 1$
4.	$\mathbf{p} \leftarrow \mathbf{H}^T\mathbf{r}^{(t-1)}, J_0 \leftarrow \arg\max_{2N_a}(\mathbf{p})$
5.	$\Lambda_t \leftarrow J_0 \cup \Lambda_{t-1}, \mathbf{A}_t = \mathbf{H}_{J_0} \cup \mathbf{A}_{t-1}$
6.	$\hat{\mathbf{x}}_t = \arg\min \| \mathbf{y} - \mathbf{A}_t\mathbf{x} \|_2^2 = (\mathbf{A}_t^T\mathbf{A}_t)^{-1}\mathbf{A}_t^T\mathbf{y}$
7.	$\hat{\mathbf{x}}_{tk} \leftarrow \arg\max_{2N_a} \| \hat{\mathbf{x}}_t \|, \Lambda_t \leftarrow \Lambda_{tk}$
8.	$\mathbf{r}_t = \mathbf{y} - \mathbf{A}_{tk}\hat{\mathbf{x}}_{tk}$
9.	end while

OMP algorithm in Table I, the inner product of measurement matrix $\mathbf{H}$ and residual $\mathbf{r}$ is calculated in each iteration and is denoted as $\mathbf{p}$, then the position of the maximum absolute value of vector $\mathbf{p}$ is found and put into the set $\mathbb{S}_t$, and then the index set Λ_t and atomic support set matrix $\mathbf{A}_t$ are updated. Additionally, $\mathbf{H}_{\Lambda_t}$ denotes a submatrix of $\mathbf{H}$ with columns indices defined by the set Λ_t, and $(\cdot)^T$ denotes the transpose of a matrix or vector. Then, the least squares method is utilized to estimate the signal $\hat{\mathbf{x}}_t$, and the residual is finally updated. The above process is repeated until the end of the iteration of the OMP algorithm. CoSaMP algorithm is an improvement edition of the basic OMP, the main difference between CoSaMP and OMP lies in each iteration, CoSaMP finds the positions of $2N_a$ values with the largest absolute values in the inner product vector, while it is 1 of the OMP. Thus, the maximum N_a absolute values in $\hat{\mathbf{x}}_t$ and their corresponding positions (eliminating the wrong atoms) are selected by exploiting the least squares method, and finally, the index set and residual are updated. The detailed steps of these two algorithms are presented in Table I and Table II, respectively.

Furthermore, a novel efficient detection algorithm combined with OMP and ML (OMP-ML) is proposed, which is specifically demonstrated as follows: in each iteration, to carry out signal estimation and residual update, K columns that are most relevant to matrix $\mathbf{H}$ are selected to put into an index set. After N_a iterations, there will be N_a index sets, and each index set contains K elements. Then, N_a elements are randomly selected from all KN_a elements, and the number of combinations will not exceed $\binom{KN_a}{N_a}$. Among these combinations, the optimal combination of activated antennas is then be determined by ML approach. Different from OMP, in the present scheme, the selection of multiple relevant atomic has a high probability to include the index of the activated antenna, and then the traversal search will be carried out on

TABLE III
OMP-ML ALGORITHM IN GSSK-VLC

Input:	$\mathbf{H}, \mathbf{y}, N_a, K$
Output:	I
1.	$\mathbf{r}_0 \leftarrow \mathbf{y}, t \leftarrow 0, \Lambda_0 \leftarrow \varnothing, \mathbf{A}_0 \leftarrow \varnothing, \Gamma_0 \leftarrow \varnothing$
2.	while $t \leq N_a$ do
3.	$t \leftarrow t + 1$
4.	$\mathbf{p} \leftarrow \mathbf{H}^T \mathbf{r}^{(t-1)}, \lambda_t \leftarrow \arg\max_K(\mathbf{p}), i_t \leftarrow \arg\max(\mathbf{p})$
5.	$\Lambda_t = i_t \cup \Lambda_{t-1}, \mathbf{A}_t = \mathbf{H}_{\Lambda_t} \cup A_{t-1}, \Gamma_t \leftarrow \Gamma_{t-1} \cup \lambda_t$
6.	$\hat{\mathbf{x}}_t = \arg\min \parallel \mathbf{y} - \mathbf{A}_t \mathbf{x} \parallel_2^2 = (\mathbf{A}_t^T \mathbf{A}_t)^{-1} \mathbf{A}_t^T \mathbf{y}$
7.	$\mathbf{r}_t = \mathbf{y} - \mathbf{A}_t \hat{\mathbf{x}}_t$
8.	end while
9.	$\mathcal{B} = \binom{\Gamma_t}{k}$
10.	$\hat{I} \leftarrow \arg\max_{\Delta \in \mathcal{B}} \parallel \mathbf{y} - \mathbf{H}\mathbf{x}_\Delta \parallel_2^2$

TABLE IV
SPARSITY AIDED SIGNAL DETECTION ALGORITHM WITH SVD
PREPROCESSING

Input:	Randomly generated bitstream $\rightarrow \{0, 1, 0, 0...\}$
Output:	Recovered bitstream
1.	bt=$\lfloor \log 2(\text{nchoosek}(N_t, N_a)) \rfloor$, com=nchoosek$(N_t, N_a)$, com=com$(1 : 2^{\text{bt}}, :)$
2.	bits $\rightarrow \underbrace{\{0, 1, 0, 0...\}}_{\text{bt}}$
3.	GSSK Modulation: Generating transmit signal $\mathbf{x}$
4.	$\mathbf{y} = \mathbf{H}\mathbf{x}, [\mathbf{y}_{\text{SVD}}, \mathbf{H}_{\text{SVD}}] = \text{SVD}(\mathbf{y}, \mathbf{H})$
5.	$(\hat{I}) = \text{OMP}(\mathbf{H}_{\text{SVD}}, \mathbf{y}_{\text{SVD}}, N_a)/\text{CoSaMP}(\mathbf{H}_{\text{SVD}}, \mathbf{y}_{\text{SVD}}, N_a)$ $/\text{OMP-ML}(\mathbf{H}_{\text{SVD}}, \mathbf{y}_{\text{SVD}}, N_a)$
6.	[idx, ia, ib] = intersect$(\hat{I}, \text{com}, \text{'rows'})$ if isempty (idx) recovered bits= $\widetilde{\text{bits}}$ else recovered bits=de2bi(ib - 1, bt, 'left-msb') end
7.	BER = biterr(bits, recovered bits)

TABLE V
SIMULATION PARAMETERS

Simulation setup	
Room size ($L \times W \times H$)	$5 \times 5 \times 3$ m^3
Number of LEDs	$9; 25; 64$
Number of PDs	$4; 16; 36$
LEDs height	3 m
PDs height	0.85 m
LEDs deployment area	$[2.1 : 0.2 : 3.5]$ m; $[2.1 : 0.3 : 3.3]$ m
PDs deployment area	$[2.4 : 2.6]$ m
Semi-angle at half power ($\Phi_{1/2}$)	$15°$
Physical area of a PD (A_{PD})	1.0 cm^2
Receiver FoV semi-angle (Ψ_{FoV})	$30°$

the candidate index set by iteration. Consequently, compared with the traditional OMP algorithm, the proposed OMP-ML algorithm can improve the reconstruction performance. It should be noted that parameter K determines the complexity and performance of the proposed OMP-ML algorithm. Specifically, when $K = 2N_a$, the detection performance and complexity have a good compromise. This conclusion draws from two aspects. At first, for OMP aided detection algorithm, only the most relevant atoms are selected as the index set of the active antenna in each iteration. In practical applications, when the quality of the signal is poor, the index of the active antenna may not be found accurately by OMP detector. As an improvement edition of the OMP detection algorithm, the proposed OMP-ML detector selects K most correlated atoms each time, and to a certain extent, the activated index position is more likely to be included. Thus, KN_a indices are obtained after N_a iterations. Then, by traversing all possible combinations, N_a indices are selected from these KN_a candidates to obtain the optimal active antenna indices. Hence, in terms of complexity, the larger the value of K, the more times of traversal will be required, and hence the computational complexity will increase. Additionally, due to the characteristics of OMP algorithm, the positions of elements with large inner product absolute value are that with strong correlations of the residual vector and the columns of measurement matrix in each iteration. Thus, these positions are more likely to contain the active antenna indices. Therefore, it is meaningless to select too large K value, which may cause conspicuous increase of the computational complexity without considerable improvement in performance. While, when the value of K is very small, the probability that the selected index set containing the index of the active antenna will be decreased during the iteration. In conclusion, in order to obtain ideal system performance, the selection of K value should be moderate. From extensive simulations, when K is $2N_a$, the algorithm performs well both in computational complexity and systematical performance. The detailed steps of the proposed algorithm are depicted in Table III.

Against the above discussion, combined with SVD preprocessing, we propose a type of sparsity signal detection algorithm to implement GSSK signal detection for the considered indoor VLC system in Table IV.

IV. SIMULATION AND NUMERICAL RESULTS

In this section, three proposed signals detection algorithms, OMP-ML, OMP and CoSaMP are utilized to demodulate GSSK signals in the considered indoor GSSK-VLC system. For comparison, the ML detection method is also considered in all simulations. The performance is measured by BER. Meanwhile, the computational complexity is also discussed in detail. In all the following simulations, the value of K in OMP-ML algorithm is set as $2N_a$.

A. Detection Performance Analysis of Indoor GSSK-VLC System

In this subsection, we will validate the performance of our proposed sparsity aided signal detection algorithms of the considered indoor GSSK-VLC system. Unless specially noted, we assume that the number of activated antennas is $N_a = 2$. The performance of ML detection and sparse reconstruction detection algorithms will be considered in the simulation with different number of LEDs and PDs, the main system simulation parameters for GSSK-VLC system are shown in the Table V.

In order to ensure that the sparsity aided detection algorithms can be utilized effectively, it is necessary to ensure that the measurement matrix $\mathbf{H}$ meets the RIP property. Therefore, when implementing the detection algorithm based on sparsity,

the channel matrix $\mathbf{H}$ needs to be preprocessed by SVD before a sparse reconstruction algorithm is executed.

To investigate the effectiveness of the measurement matrix preprocessing method proposed in this paper, the detection performance of sparsity aided algorithm with and without SVD preprocessing on measurement matrix $\mathbf{H}$ is demonstrated below. Fig. 4 depicts the detection results without measurement matrix preprocessing, where $N_t = 64$ and $N_r = 36$ for the considered indoor GSSK-VLC system. Observed from the simulation results that upon increasing the SNR, all sparsity aided signal detection algorithms fail to detect GSSK signals and the BER tend to a constant value, which indicates that the greedy algorithm based on CS sparse reconstruction is almost unable to reconstruct the original signal if there is no preprocessing operation on measurement matrix. However, the ML detection approach can detect the GSSK signals successfully upon increasing SNR.
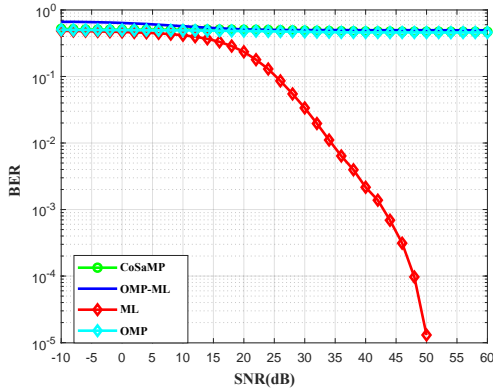

Fig. 4. BER performance of ML detection algorithm and CS aided detection algorithms without SVD preprocessing with configuration $N_t = 64$, $N_r = 36$.

Then, to demonstrate the efficiency of the proposed preprocessing approach and detection algorithms, we consider a special case of GSSK modulation with $N_a = 1$ (i.e. SSK modulation), where the performance of each detection algorithm with different $\Phi_{1/2}$ is considered. In the simulation, the numbers of N_t and N_r are set to 9 and 4, respectively, LEDs are uniformly distributed in the $[0.6, 2.6] \times [0.6, 2.6]$ m^2 area, and PDs are uniformly distributed in the $[2.4, 2.6] \times [2.4, 2.6]$ m^2 area. As shown in Fig. 5, when measurement matrix $\mathbf{H}$ is preprocessed to satisfy the RIP property, the performance of sparsity aided algorithm is significantly improved, and the proposed OMP-ML algorithm provide the best BER performance. Moreover, it can also be seen that the detection performance enhances as the increase of $\Phi_{1/2}$. However, for ML detection, the detection performance decrease upon increasing $\Phi_{1/2}$.

Let us now focus on GSSK situation. We consider the following two scenarios: 1) $N_t = 25$, $N_r = 16$, the LEDs are uniformly distributed in the $[2.1, 3.3] \times [2.1, 3.3]$ m^2 region with an interval of 0.3 m of adjacent two LEDs; 2) $N_t = 64$, $N_r = 36$, the LEDs are uniformly distributed in the $[2.1, 3.5] \times [2.1, 3.5]$ m^2 region, and the LED interval is 0.2 m of adjacent two LEDs. In all simulations, the user's PDs
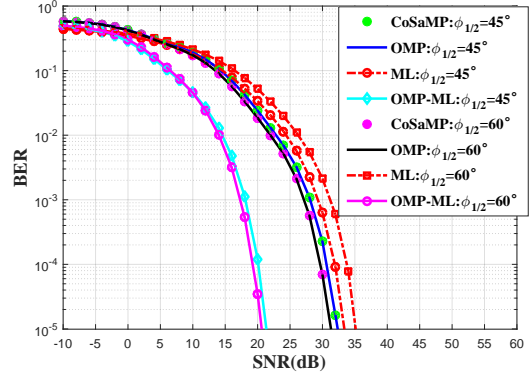

Fig. 5. BER performance of ML detection and CS aided detection algorithms with SVD preprocessing, where $N_t = 9$, $N_r = 4$, $\Phi_{1/2} = 45°, 60°$.

positions are fixed within the range of $[2.4, 2.6] \times [2.4, 2.6]$ m^2. Fig. 6 depicts the BER performance of ML, OMP-ML, OMP and CoSaMP detection algorithms with different SNRs. From Fig. 6, it can be seen that the BER performance of OMP algorithm is poor and affected by floor effect, while both OMP-ML and CoSaMP algorithms can detect the original GSSK signals efficiently. Additionally, we can observe from Fig. 6 that the ML detection approach can also detect the GSSK signals properly. Furthermore, the BER performance gap between ML and CoSaMP detection algorithms is almost 36 dB and 26 dB when BER is 10^{-5} with configurations $N_t = 64, N_r = 36$ and $N_t = 25, N_r = 16$, respectively.
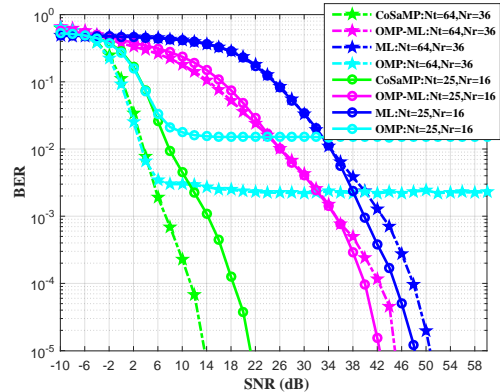

Fig. 6. BER performance of ML detector and CS aided detection algorithms with SVD preprocessing, where $N_t = 64$, $N_r = 36$ and $N_t = 25$, $N_r = 16$, respectively.

From Fig. 6, we can also learn that the performance of three sparsity based detection algorithms is improved upon increasing the number of LEDs at the transmitter, and the performance improvement of CoSaMP is more obvious than that of OMP-ML and OMP. However, the performance of ML detector is deteriorated with the increase of the number of LEDs, because the increase of the number of LEDs will bring more serious interference and stronger correlation of channels, which results in performance loss of ML detection method.

Actually, this is determined by the detection characteristics of ML. However, for sparsity aided detection algorithms, with the increase of the number of LEDs, the transmitted signals become more sparser, which results in the improved detection performance.

It can also be seen from the simulation results in Fig. 6 that CoSaMP algorithm has more obvious advantages in GSSK-VLC system as N_t increases. This is because the backtracking mechanism is adopted by CoSaMP algorithm, and the operation of elimination wrong selected atoms in each iteration can potentially improve the accuracy of signal reconstruction. Therefore, the CoSaMP significantly outperforms other non-backtracking sparsity aided greedy algorithms.

Fig. 7 depicts the performance for ML algorithm and our proposed sparsity aided signal selection algorithms OMP, CoSaMP and OMP-ML for the investigated two cases, where we have $N_t = 64$, $N_r = 25$ and $N_t = 64, N_r = 36$ for the indoor GSSK-VLC system. Observe that the performance of the three sparsity aided detection algorithms is significantly improved upon increasing the number of PDs at the receiver, and the performance enhancement of ML detection method is limited. Additionally, the floor effect of the performance of OMP-ML and CoSaMP detection algorithms can be effectively alleviated as the number of PDs increasing.
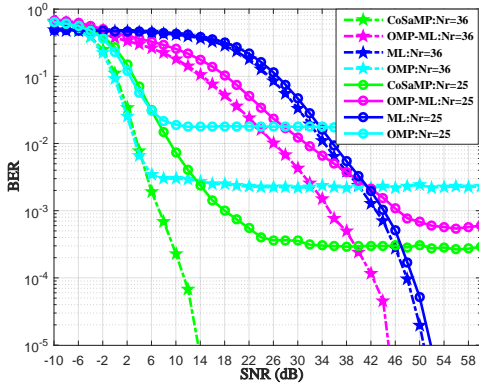

Fig. 7. BER performance of ML detector and CS aided detection algorithms with SVD preprocessing vs. N_r, where $N_t = 64$, $N_r = 25, 36$.

Finally, it can be seen from the simulation results that the sparsity aided detection algorithm has better performance than that of the ML detector. The main reason is that the detection principles of the two types of detection algorithms are different. Specifically, the sparse signal reconstruction algorithm based on CS filters out the noise of some non-sampling points when doing relevant sparse sampling or preprocessing the measurement matrix, while the principle of ML detection algorithm is through exhaustive search and enumeration. Consequently, when the signal to be recovered is sparse enough and the channel itself has poor quality, the non-sampling point (the position of the zero-value) will be added into certain amount of noise, which causes the detection performance of ML sharply declined. At the same time, in our considered indoor GSSK-VLC system, the signals to be transmitted has strong sparsity when the number of LEDs at

TABLE VI
COMPUTATION COMPLEXITY ANALYSIS OF VARIOUS DETECTORS FOR INDOOR GSSK-VLC SYSTEM IN TERMS OF FLOPS

Detection algorithm	Real-valued flops
ML	$(2N_r N_t + 2N_r - 1)2^B$
OMP	$N_a N_t (2N_r - 1) + 23N_r + 5$
OMP-ML	$N_a N_t (2N_r - 1) + 5N_r + N_r N_a (4N_a + 1) + 2N_a^3 - N_a^2 - N_a + (2N_r N_t + 2N_r - 1)\binom{K N_a}{N_a}$
CoSaMP	$N_r N_a (2N_t + 48N_a^2 + 7N_a) - N_a (13N_a^2 + N_t - 21N_a - 525) - 808$

the transmitter is large, and consequently the sparsity aided detection algorithms have better performance than that of the ML detector.

B. Complexity analysis

Because the signals and elements of channel matrices in indoor VLC system are both positive real numbers. In this paper, we will analyze the complexity of ML detection algorithm as well as the proposed sparsity aided signal detection algorithms: OMP-ML, OMP and CoSaMP from the perspective of floating point operations (flops). The specific complexity calculation is shown in Table VI.
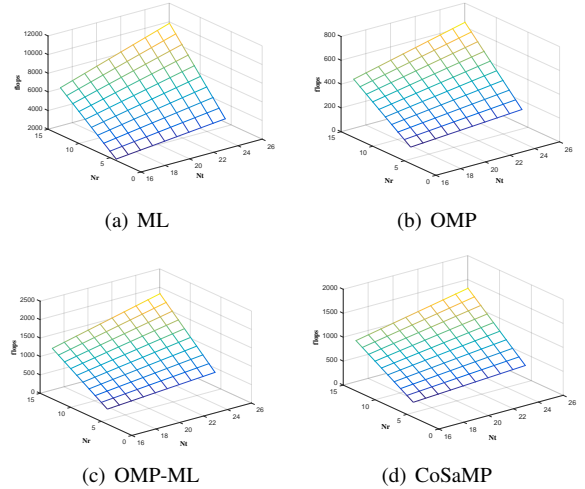

(a) ML

(b) OMP

(c) OMP-ML

(d) CoSaMP

Fig. 8. The number of flops of various detection algorithms as a function of N_t and N_r in SSK-VLC system with $N_a = 1$ (a) ML; (b) OMP; (c) OMP-ML; (d) CoSaMP.

It should be noted that, the computation complexity of SVD is $4N_t^2 N_r + 22N_r^3$, furthermore, the SVD preprocessing needs only one operation. In the simulation process, the number of symbols is set to 10^5, and the number of flops of ML is $10^5(2N_r N_t + 2N_r - 1)2^B$. Thus, the complexity of SVD here is negligible.

Note also that the parameters utilized in complexity analysis are the same as previous simulations as seen in Table V. In ML detection algorithm, parameter B represents the spectrum efficiency of the system. Additionally, in the simulation process, the iteration number of sparsity aided algorithms are all set as the number of active antennas N_a. In Table VII, the number of real-valued flops required by the CS aided detection algorithms and the ML detector under different N_t
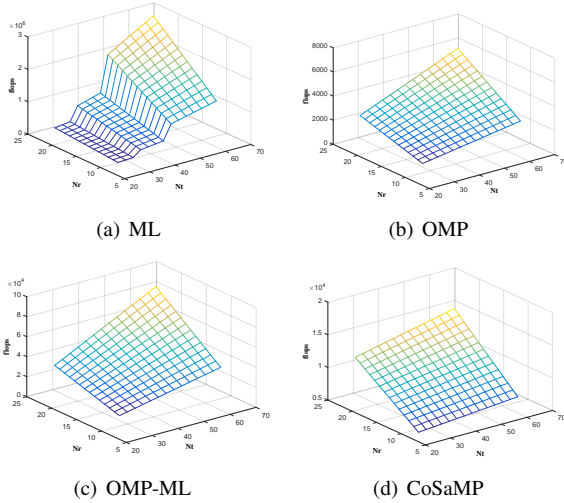
(a) ML

(b) OMP

(c) OMP-ML

(d) CoSaMP

Fig. 9. The number of flops of various detection algorithms as a function of N_t and N_r in GSSK-VLC system with $N_a = 2$ (a) ML; (b) OMP; (c) OMP-ML; (d) CoSaMP.

TABLE VII
FLOPS OF VARIOUS ALGORITHMS AND THE COMPLEXITY REDUCTION RATES WITH RESPECT TO ML DETECTOR WITH DIFFERENT PARAMETER SETTINGS

$N_t = 64, N_r = 36$				
Detector	OMP	CoSaMP	OMP-ML	ML
flops	9921	24142	140938	4797296
Reduction rate	99%	99%	97%	0%
$N_t = 36, N_r = 25$				
Detector	OMP	CoSaMP	OMP-ML	ML
flops	4108	14050	55885	946688
Reduction rate	99%	97%	94%	0%

and N_r settings are presented when $N_a = 2$, including real-valued multiplications and real-valued additions. Furthermore, the complexity reduction rates with respect to ML detector of different detectors are also given. Fig. 8 and Fig. 9 shows the number of flops of various algorithms as a function of N_t and N_r when $N_a = 1$ and 2, respectively. Subsequently, when $N_t = 25, 36, 64$ and $N_r = 16$, the actual running time of each detection algorithm are demonstrated in Fig. 10.
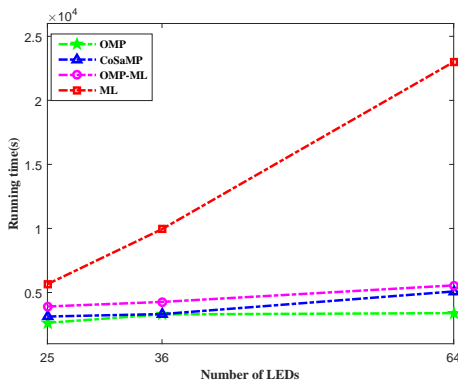

Fig. 10. Running time of ML and sparsity aided detection algorithms with SVD preprocessing as a function of N_t in GSSK system, where $N_t = 25, 36, 64$.

As can be seen from Fig. 8 to Fig. 10, ML detector has the highest complexity compared with sparsity aided algorithms under the same parameters setting, which also indicates that the sparsity aided signal detection algorithm is more suitable for large-scale MIMO scenarios with a large number of transmitting LEDs. Furthermore, the actual running time also validates our theoretical analysis.

V. CONCLUSION

In this paper, aiming at the problem of detection GSSK modulation signals in indoor VLC system, we propose a class of sparsity aided signal detection algorithms based on CS, which mainly solves the following two issues. Firstly, the SVD based preprocessing of the measurement matrix is proposed to enable the measurement matrix to meet the RIP property, which lays a theoretical foundation for the following signal detection methods based on CS sparse reconstruction algorithm. We characterize that, without special preprocessing strategy, the sparsity aided detection cannot work well. Then, three sparse detection algorithms for GSSK modulation signals in indoor VLC system are proposed, which are termed as OMP-ML, OMP and CoSaMP. This type of algorithm is fundamentally different from the ML based detection algorithm in principle, so as to effectively improve the BER performance and reduce the computational complexity in MIMO-VLC system. Through theoretical analysis and simulation results, the sparse signal detection scheme based on SVD measurement matrix preprocessing proposed can provide lower BER performance imposed by a lower computational complexity, which is especially suitable for MIMO system with a large number of LEDs.

REFERENCES

[1] N. Chi, Y. Zhou, Y. Wei, and F. Hu, "Visible light communication in 6G: Advances, challenges, and prospects," *IEEE Vehicular Technology Magazine*, vol. 15, no. 4, pp. 93–102, Dec. 2020.

[2] X. Deng, K. Arulandu, Y. Wu, S. Mardanikorani, G. Zhou, and J. M. G. Linnartz, "Modeling and analysis of transmitter performance in visible light communications," *IEEE Transactions on Vehicular Technology*, vol. 68, no. 3, pp. 2316–2331, Mar. 2019.

[3] R. Mitra and V. Bhatia, "Minimum error entropy criterion based channel estimation for massive-MIMO in VLC," *IEEE Transactions on Vehicular Technology*, vol. 68, no. 1, pp. 1014–1018, Jan. 2019.

[4] R. Y. Mesleh, H. Haas, S. Sinanovic, C. W. Ahn, and S. Yun, "Spatial modulation," *IEEE Transactions on Vehicular Technology*, vol. 57, no. 4, pp. 2228–2241, Jul. 2008.

[5] M. Wen, B. Zheng, K. J. Kim, M. Di Renzo, T. A. Tsiftsis, K.-C. Chen, and N. Al-Dhahir, "A survey on spatial modulation in emerging wireless systems: Research progresses and applications," *IEEE Journal on Selected Areas in Communications*, vol. 37, no. 9, pp. 1949–1972, Sep. 2019.

[6] J. Jeganathan, A. Ghrayeb, L. Szczecinski, and A. Ceron, "Space shift keying modulation for MIMO channels," *2009 IEEE Transactions on Wireless Communications*, vol. 8, no. 7, pp. 3692–3703, Jul. 2009.

[7] J. Jeganathan, A. Ghrayeb, and L. Szczecinski, "Generalized space shift keying modulation for MIMO channels," in *2008 IEEE 19th International Symposium on Personal, Indoor and Mobile Radio Communications*, Sep. 2008, pp. 1–5.

[8] A. Younis, N. Serafimovski, R. Mesleh, and H. Haas, "Generalised spatial modulation," in *2010 Conference Record of the Forty Fourth Asilomar Conference on Signals, Systems and Computers*, Nov. 2010, pp. 1498–1502.

[9] L.-L. Yang, "Transmitter preprocessing aided spatial modulation for multiple-input multiple-output systems," in *2011 IEEE 73rd Vehicular Technology Conference (VTC Spring)*, Jul. 2011, pp. 1–5.

[10] R. Zhang, L.-L. Yang, and L. Hanzo, "Generalised pre-coding aided spatial modulation," *IEEE Transactions on Wireless Communications*, vol. 12, no. 11, pp. 5434–5443, Nov. 2013.

[11] R. Mesleh, S. S. Ikki, and H. M. Aggoune, "Quadrature spatial modulation," *IEEE Transactions on Vehicular Technology*, vol. 64, no. 6, pp. 2738–2742, Jan. 2015.

[12] J. Li, M. Wen, X. Cheng, Y. Yan, S. Song, and M. H. Lee, "Generalized precoding-aided quadrature spatial modulation," *IEEE Transactions on Vehicular Technology*, vol. 66, no. 2, pp. 1881–1886, Feb. 2017.

[13] J. Li, S. Dang, Y. Yan, Y. Peng, S. Al-Rubaye, and A. Tsourdos, "Generalized quadrature spatial modulation and its application to vehicular networks with noma," *IEEE Transactions on Intelligent Transportation Systems*, vol. 22, no. 7, pp. 4030–4039, Jul. 2021.

[14] M. D. Renzo, H. Haas, A. Ghrayeb, S. Sugiura, and L. Hanzo, "Spatial modulation for generalized MIMO: Challenges, opportunities, and implementation," *Proceedings of the IEEE*, vol. 102, no. 1, pp. 56–103, Jan. 2014.

[15] W. O. Popoola, E. Poves, and H. Haas, "Error performance of generalised space shift keying for indoor visible light communications," *IEEE Transactions on Communications*, vol. 61, no. 5, pp. 1968–1976, May 2013.

[16] W. O. Popoola and H. Haas, "Demonstration of the merit and limitation of generalised space shift keying for indoor visible light communications," *Journal of Lightwave Technology*, vol. 32, no. 10, pp. 1960–1965, May 2014.

[17] Q. Zhang, Z. Bai, N. Zhang, S. Sun, and K. S. Kwak, "Performance analysis of DC-SSK scheme and its power allocation in VLC system," in *2018 International Conference on Computing, Networking and Communications (ICNC)*, Mar. 2018, pp. 280–284.

[18] F. Wang, C. Liu, Q. Wang, J. Zhang, R. Zhang, L. Yang, and L. Hanzo, "Secrecy analysis of generalized space-shift keying aided visible light communication," *IEEE Access*, vol. 6, pp. 18 310–18 324, Jan. 2018.

[19] ——, "Optical jamming enhances the secrecy performance of the generalized space-shift-keying-aided visible-light downlink," *IEEE Transactions on Communications*, vol. 66, no. 9, pp. 4087–4102, Sep. 2018.

[20] Z. Gao, L. Dai, C. Qi, C. Yuen, and Z. Wang, "Near-optimal signal detector based on structured compressive sensing for massive SM-MIMO," *IEEE Transactions on Vehicular Technology*, vol. 66, no. 2, pp. 1860–1865, Feb. 2017.

[21] M. Wen, J. Li, S. Dang, Q. Li, S. Mumtaz, and H. Arslan, "Joint-mapping orthogonal frequency division multiplexing with subcarrier number modulation," *IEEE Transactions on Communications*, vol. 69, no. 7, pp. 4306–4318, Jul. 2021.

[22] D. L. Donoho, "Compressed sensing," *IEEE Transactions on Information Theory*, vol. 52, no. 4, pp. 1289–1306, Apr. 2006.

[23] J. A. Tropp and A. C. Gilbert, "Signal recovery from random measurements via orthogonal matching pursuit," *IEEE Transactions on Information Theory*, vol. 53, no. 12, pp. 4655–4666, Dec. 2007.

[24] D. Needell and J. Tropp, "CoSaMP: Iterative signal recovery fromincomplete and inaccurate samples," *Applied and Computational Harmonic Analysis*, vol. 26, no. 3, pp. 301–321, May 2009.

[25] C. Yu, S. Hsieh, H. Liang, C. Lu, W. Chung, S. Kuo, and S. Pei, "Compressed sensing detector design for space shift keying in MIMO systems," *IEEE Communications Letters*, vol. 16, no. 10, pp. 1556–1559, Oct. 2012.

[26] C. Wu, W. Chung, and H. Liang, "OMP-based detector design for space shift keying in large MIMO systems," in *2014 IEEE Global Communications Conference*, Dec. 2014, pp. 4072–4076.

[27] S. Kallummil and S. Kalyani, "Combining ml and compressive sensing: Detection schemes for generalized space shift keying," *IEEE Wireless Communications Letters*, vol. 5, no. 1, pp. 72–75, Feb. 2016.

[28] X. Zhang, Q. Liu, and M. Jin, "Detection of generalized space shift keying signal with sparse reconstruction," *IEEE Transactions on Vehicular Technology*, vol. 66, no. 6, pp. 5471–5475, June 2017.

[29] L. C. Zhang, S. N. Zhu, L. J. Zhang, and L. M. Jin, "Low-complexity sparse detector for generalised space shift keying," *Electronics Letters*, vol. 55, no. 5, pp. 268–270, Mar. 2019.

[30] K. Gligoric, M. Ajmani, D. Vukobratovic, and S. Sinanovic, "Visible light communications-based indoor positioning via compressed sensing," *IEEE Communications Letters*, vol. 22, no. 7, pp. 1410–1413, Jul. 2018.

[31] M. K. A. Sezer and S. Gezici, "Localization via visible light systems," *Proceedings of the IEEE*, vol. 106, no. 6, pp. 1063–1088, Jun. 2018.

[32] B. Lin, Z. Ghassemlooy, J. Xu, Q. Lai, X. Shen, and X. Tang, "Experimental demonstration of compressive sensing-based channel estimation for MIMO-OFDM VLC," *IEEE Wireless Communications Letters*, vol. 9, no. 7, pp. 1027–1030, Jul. 2020.

[33] L. An, H. Shen, J. Wang, Y. Zeng, and R. Ran, "Energy efficiency optimization for MIMO visible light communication systems," *IEEE Wireless Communications Letters*, vol. 9, no. 4, pp. 452–456, Apr. 2020.

[34] X. Gao, Z. Bai, P. Gong, and D. O. Wu, "Design and performance analysis of led-grouping based spatial modulation in the visible light communication system," *IEEE Transactions on Vehicular Technology*, vol. 69, no. 7, pp. 7317–7324, Jul. 2020.

[35] Y. X. Gong, L. W. Ding, Y. J. He, H. B. Zhu, and Y. J. Wang, "Analysis of space shift keying modulation applied to visible light communications," in *IET International Conference on Information and Communications Technologies (IETICT 2013)*, Apr. 2013, pp. 503–507.

[36] E. J. Candes and M. B. Wakin, "An introduction to compressive sampling," *IEEE Signal Processing Magazine*, vol. 25, no. 2, pp. 21–30, Mar. 2008.

[37] E. J. Candes, "Compressive sampling," *Marta Sanz Sole*, vol. 17, no. 2, pp. 1433–1452, Jan. 2006.

[38] C. M. Jarque and A. K. Bera, "A test for normality of observations and regression residuals," *International Statistical Review/Revue Internationale de Statistique*, pp. 163–172, 1987.